The Monashee reflection: Re-examination of a Lithoprobe crustal-scale seismic reflection in the southern Canadian Cordillera

Stefan Kruse
Paul F. Williams*
Department of Geology, University of New Brunswick, P.O. Box 4400, Fredericton NB E3B 5A3, Canada

ABSTRACT

The Monashee reflection is a major crustal-scale, crosscutting reflection that appears on two mutually perpendicular Lithoprobe seismic profiles in the southern Omineca belt of the Canadian Cordillera. It has previously been interpreted as the down-plunge extension of a regional ductile thrust fault, the Monashee décollement, which is said to separate the Monashee complex from the overlying Selkirk allochthon. We reinterpret the Monashee reflection as a shear zone with modest, normal displacement based on recent mapping, geometric analysis of the seismic profiles, and existing geochronological and metamorphic data.

Recent mapping has demonstrated that this boundary is not a shear zone with thrust geometry, but rather it is a gradational boundary that has resulted from mutual folding and transposition of rocks ascribed to the Monashee complex and Selkirk allochthon. Overprinting the transition zone in different areas are three high-strain zones: the Greenbush Lake shear band zone, Slate Mountain shear zone, and a ductile shear zone associated with the Columbia River fault. We interpret these high-strain zones as segments of a single, high-strain zone that wraps around the margins of the Thor-Odin culmination. This marginal zone is a complex, outward-dipping, normal structure, which we name the Thor-Odin high-strain zone.

Three alternative three-dimensional geometric models have been developed for the Monashee reflection in order to project the reflection to the surface. We favor a model in which the surface trace of the Monashee reflection coincides with the Thor-Odin high-strain zone.

Normal shear sense kinematics are interpreted for the Monashee reflection based on: (1) the overall geometry and fault-drag–like relationship between the Monashee reflection and reflections in the hanging wall and footwall; (2) offset of metamorphic and geochronological gradients, which are consistent with an extensional zone rather than with a thrust fault interpretation; and (3) the crosscutting nature of the Monashee reflection, which is consistent with normal structures throughout the region.

Keywords: structure, Lithoprobe, seismic-reflection profiles, Monashee complex, Cordillera.

INTRODUCTION

The Shuswap complex is a fault-bounded high-grade terrane within the southern Omineca belt of the Canadian Cordillera (Fig. 1). It is defined by Eocene normal faults or shear zones that juxtapose low-grade, upper-crustal assemblages in the hanging walls with greenschist to amphibolite facies, middle-crustal and basement-zone rocks in the footwalls (Brown and Read, 1983; Brown and Journeay, 1987; Carr, 1991; Bardoux and Mareschal, 1994; Carr, 1995; Johnson and Brown, 1996; Johnson, 2006).

The Monashee complex is a structural culmination within the Shuswap complex that exposes Proterozoic North American basement rocks (Armstrong, 1982; Parrish and Armstrong, 1983; Armstrong et al., 1991; Crowley, 1999). It is composed of two smaller structural culminations, the northern Frenchman Cap culmination and the southern Thor-Odin culmination (Fig. 1).

Two mutually perpendicular Lithoprobe lines, composite line 7–8–9 and line 6 (Fig. 2A) were recorded south of the Thor-Odin culmination, which would allow for some three-dimensional (3-D) information to be inferred from reflections that appear on both lines. The most prominent of these reflections is the Monashee reflection, a crustal-scale discontinuity that appears as a S-plunging trace on profile 6 and as a curved and both E- and W-plunging trace on composite profile 7–8–9 (Fig. 2B). The traces intersect where the seismic lines cross, indicating that they represent a single surface.

The Monashee reflection can potentially be interpreted as: (1) a shear zone with thrust geometry (Brown et al., 1992; Cook et al., 1992; McNicoll and Brown, 1995; Varsek and Cook, 1994; Vasudevan et al., 1995); (2) the base of Mesozoic Cordilleran deformation; (3) an inherited, Proterozoic structure or contact (Thompson et al., 2002); (4) a folded extensional shear zone; or (5) a complex high-strain zone. In this contribution, we argue in favor of a complex high-strain zone origin, which would correlate the Monashee reflection with the W-dipping, normal Greenbush Lake shear band zone in the west, the S-dipping Slate Mountain shear zone in the south, and the E-dipping, normal, ductile Columbia River fault in the east. These three zones outcrop around the margins of the Thor-Odin culmination, lie on-strike of one another (Fig. 1), overprint a regional transposition foliation, and are interpreted to form a single, complex high-strain zone. We name this structure the Thor-Odin high-strain zone.

The Monashee reflection has been correlated with the Monashee décollement (Brown et al., 1992; Cook et al., 1992; Carr, 1995), which is a crustal-scale ductile shear zone with thrust kinematics that is said to separate the Monashee complex from the overlying middle and upper crustal zones (collectively known as the Selkirk allochthon) of Carr (1991). As interpreted, the Monashee décollement outcrops as an arcuate shear zone that is approximately coincident with our Thor-Odin high-strain zone. The Monashee décollement is also interpreted as linking to the basal detachment that lies below the Rocky Mountain fold-and-thrust belt (Brown et al., 1992; Cook et al., 1992). The Monashee décollement, as defined by McNicoll and Brown

*Corresponding author: pfw@unb.ca, +1-506-453-4803.

Geosphere; February 2007; v. 3; no. 1; p. 26–41; doi: 10.1130/GES00049.1; 12 figures, 3 animations.

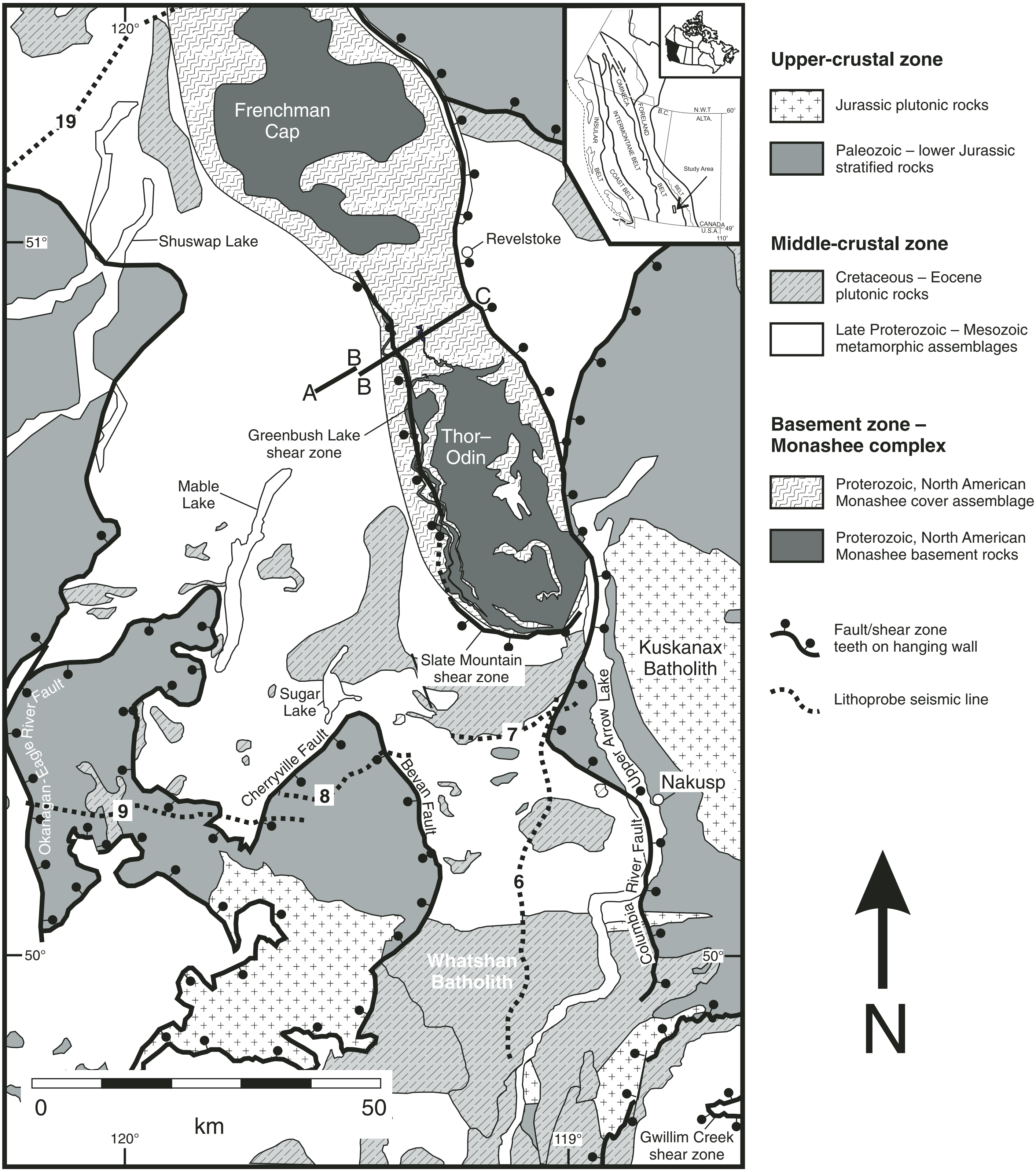

Figure 1. Geology of the southern Omineca belt modified from Carr (1991) indicating the positions of Lithoprobe seismic transects 6 and 7–8–9. Inset map shows the position of the study area with respect to the morphogeological belts of the Canadian Cordillera (Gabrielse et al., 1991). Section line A–B–C is shown in Figure 3.

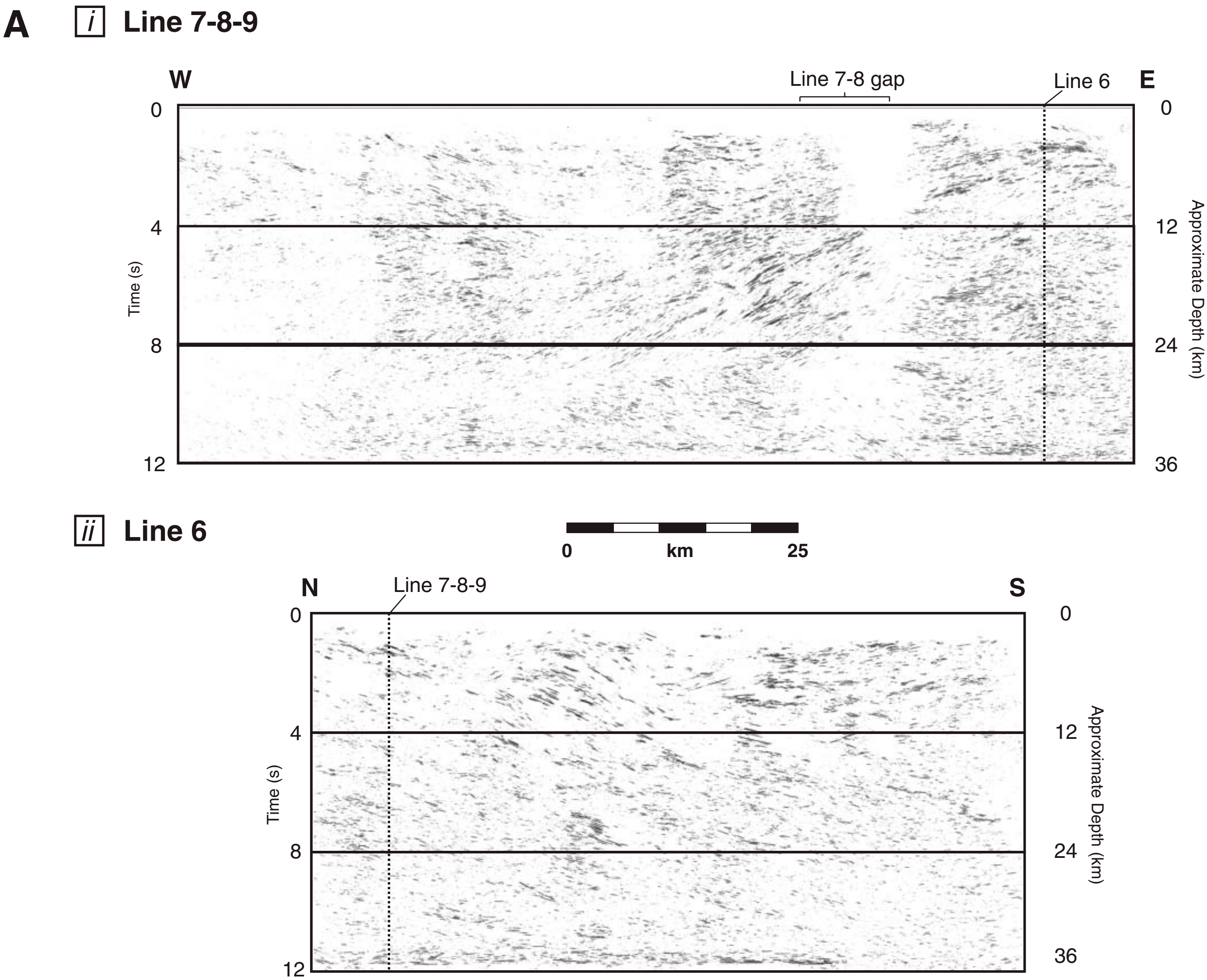

Figure 2A. Migrated and coherency filtered Lithoprobe seismic reflection profiles. Acquisition and processing parameters are given in Cook et al. (1988) and Cook et al. (1992). (i) Merged Lithoprobe seismic profiles of east-west–trending lines 7–8–9. (ii) North-south–trending Lithoprobe seismic section 6.

(1995) in the Thor-Odin culmination, is said to project into the trace of the Monashee reflection on profiles 6 and 7–8–9. In Frenchman Cap, the Monashee décollement has been projected parallel to the W-dipping seismic fabric from its interpreted surface position, down onto Lithoprobe profile 19, where it is indistinguishable as a discrete structure (Cook et al., 1992). The Monashee décollement is described as having a top-to-the-NE sense of displacement (Brown et al., 1986; Lane et al., 1989; Brown et al., 1992; Cook et al., 1992; McNicoll and Brown, 1995; Gibson et al., 1999; Crowley et al., 2001) and an estimated magnitude of displacement between 80 and 100 km (Brown et al., 1986, 1992).

Varsek and Cook (1994) reinterpreted the Lithoprobe data to correlate the Monashee reflection with the Monashee décollement, but suggested that it is the upper boundary of a 20-km-thick, W-dipping, crustal-scale thrust ramp that correlates with the Priest River ramp interpreted from Consortium for Continental Reflection Profiling (COCORP) lines in Washington State. The Monashee ramp is described as a contractional structure that has been relatively unaffected by subsequent extensional deformation (Varsek and Cook, 1994).

An alternative hypothesis is that the Monashee reflection represents a pre-Cordilleran, Proterozoic structure. Thompson et al. (2002) argued that semicontinuous stratigraphy across this portion of the southern Omineca belt precludes structures with large displacements, such as the Monashee décollement. Consequently they suggested that the deep crustal structure, inferred from Lithoprobe seismic profiles, predates the Proterozoic Belt-Purcell and younger sedimentary successions (Thompson et al., 2002). In our interpretation, the Monashee reflection is an Eocene high-strain zone with modest displacement, and thus it is not in conflict with the stratigraphic observations of Thompson et al. (2002).

In addition to the Monashee reflection, we discuss a second important reflection, the Valhalla reflection. Above the Monashee reflection, in profiles 6 and 7–8–9, there are gently undulating reflections with a horizontal enveloping surface (Fig. 2B). These have been interpreted as representing a single surface that correlates with the Valhalla reflection from Lithoprobe profile 5 (Carr, 1995). The Valhalla reflection,

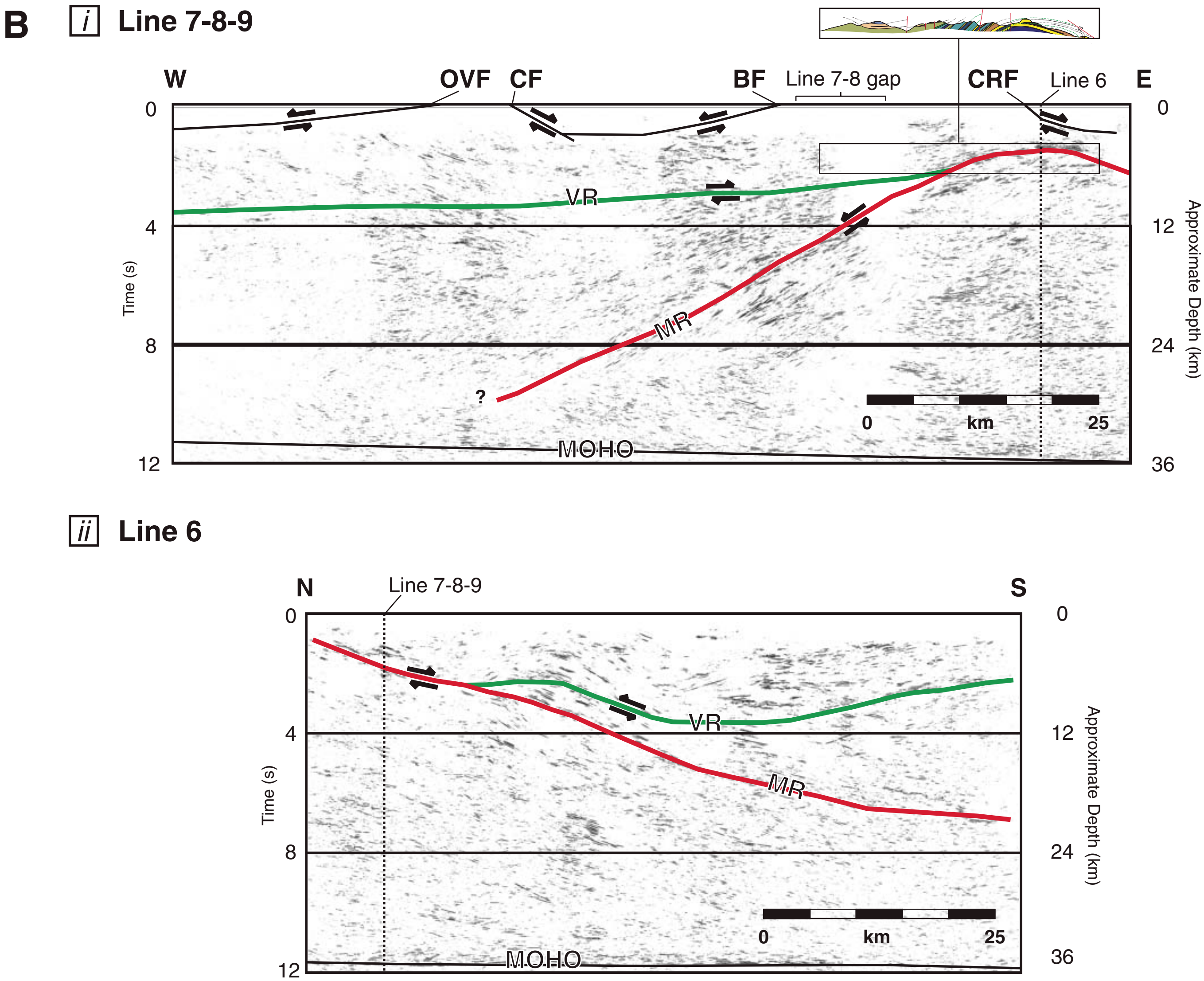

Figure 2B. Interpreted, migrated and coherency filtered Lithoprobe seismic reflection profiles. Acquisition and processing parameters are given in Cook et al. (1988, 1992). (i) Merged profile of east-west–trending sections 7–8–9 with interpreted positions of the Monashee reflection (MR), and Valhalla reflection (VR). Interpretation of the Okanagan Valley–Eagle River fault (OVF), Bevan fault (BV), Cherryville fault (CV), Columbia River fault (CRF), and Mohorovic discontinuity (MOHO) is in agreement with previous studies (Carr, 1991; Brown et al., 1992; Cook et al., 1992). Compare the geometry of the reflections in the boxed area with the simplified cross section from the western margin of the northern Thor–Odin culmination (see Figure 3 for full cross section). (ii) North-south–trending section 6, indicating the interpreted position of the MR and VR.

in turn, has been correlated with the Gwillim Creek shear zone in the Valhalla complex (Cook et al., 1988; Eaton and Cook, 1990; Cook et al., 1992; Carr, 1995).

Geology

The Monashee décollement was first mapped in Frenchman Cap and later extended to the Thor-Odin culmination (Read and Brown, 1981; Brown and Read, 1983; Journeay, 1986; Bosdachin and Harrap, 1988; Harrap, 1990; Carr, 1991; Brown et al., 1992; McNicoll and Brown, 1995). In agreement with earlier mapping (Jones, 1959; Craig, 1966; Reesor and Moore, 1971; Mutti, 1978), our mapping (Johnston, 1998; Johnston et al., 2000; Spark, 2001; Kruse et al., 2004; Williams and Jiang, 2005) has failed to reveal a shear zone with thrust geometry or other sharp separation of the Monashee complex and the Selkirk allochthon (Fig. 3).

As stated already, we do recognize a high-strain zone, the Thor-Odin high-strain zone, which wraps around the culmination from the west flank to the east flank, approximately coincident with the inferred Monashee décollement. However, this high-strain zone is not the boundary between the Monashee complex and the Selkirk allochthon, nor does it have the kinematics of a thrust.

The transition from the basement zone to middle-crustal zone is characterized by isoclinal infolding (at all scales from microscopic to regional) of basement-zone Monashee complex rocks with overlying middle-crustal zone rocks of the Selkirk allochthon (Fig. 3), such that no

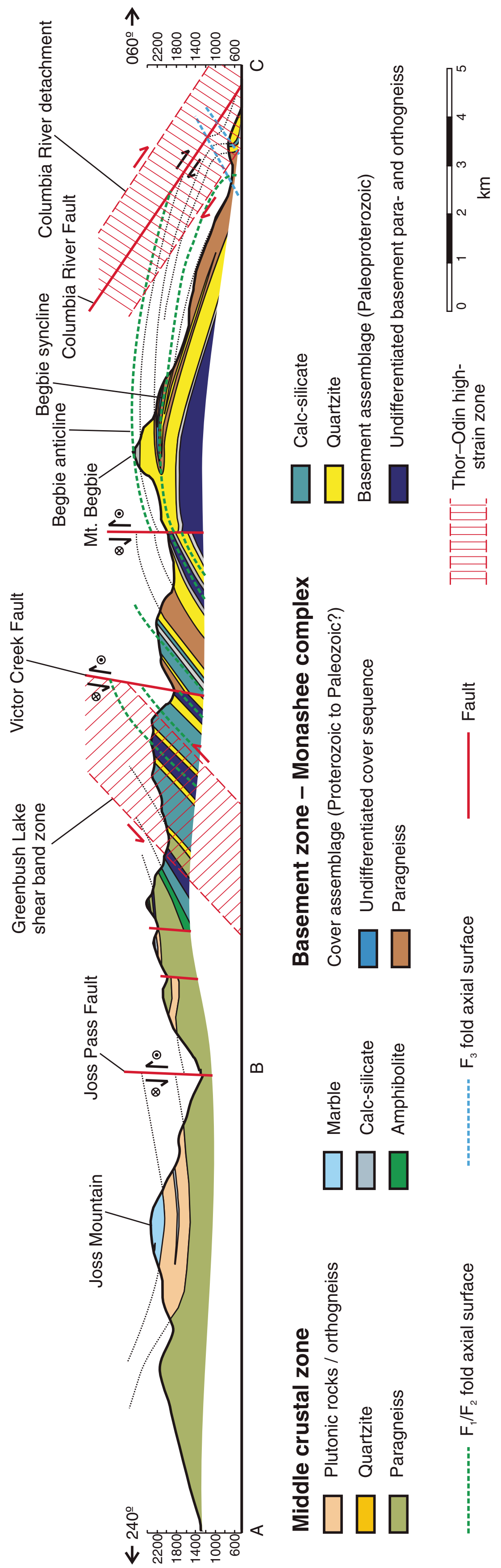

Figure 3. Cross section from the Columbia River to Joss Mountain in the northern Thor-Odin culmination and Selkirk allochthon. Monashee complex basement-zone rocks are isoclinally infolded with Selkirk allochthon middle-crustal zone rocks. This transition is overprinted by the ductile Greenbush Lake shear band zone and subsequently by brittle faults. Compare the sigmoidal deflection of the transposition foliation (S_T) across the Greenbush Lake shear band zone with the deflection of reflections adjacent to the Monashee reflection in Figure 2. Location of the section line is shown in Figure 1.

sharp break exists between the two (Johnston et al., 2000; Spark, 2001; Kruse et al., 2004). Thus, if the Monashee décollement ever existed in the Thor-Odin culmination, it must have been an early structure that is now totally obscured by transposition.

A penetrative transposition fabric (S_T) is present not only in the transition zone but throughout the Thor-Odin culmination and much of the middle-crustal zone. It is a product of penetrative noncoaxial flow with a consistent top-to-the-NE sense of shear in the Monashee complex and the lower part of the middle-crustal zone and a top-to-the-SW sense of shear at higher structural levels (Johnston et al., 2000; Williams and Jiang, 2005; Kuiper et al., 2006).

This transposed transition between basement and middle-crustal zones is subsequently overprinted by the ductile, complex Thor-Odin high-strain zone (Fig. 4). Late brittle structures subsequently overprint both the early transposition fabric (S_T) and the Thor-Odin high-strain zone (Kruse and Williams, 2005).

We have linked the previously mapped Greenbush Lake shear band zone (Johnston, 1998; Johnston et al., 2000), the Slate Mountain shear zone (Carr, 1991), and the ductile Columbia River fault (Brown and Murphy, 1981; Read and Brown, 1981; Lane et al., 1989) to form the Thor-Odin high-strain zone. We divide the Thor-Odin high-strain zone into three segments that differ from the original segments. The previously mapped arcuate Slate Mountain shear zone (Carr, 1991) includes three domains with different kinematics. The western end is on-strike with the Greenbush Lake shear band zone and contains fabrics consistent with W-side-down noncoaxial shear (Fig. 4). Therefore, we link this portion of the Slate Mountain shear zone and the Greenbush Lake shear band zone and refer to the combined normal structure as the Thor-Odin detachment (Fig. 4).

The southern, approximately east-west–trending, middle portion of the Slate Mountain shear zone (Fig. 4) is characterized by a fabric that indicates horizontal coaxial extension. We refer to this domain of E-W stretching as the Slate Mountain high-strain zone.

The east flank of the Thor-Odin culmination is bounded by the Columbia River fault (Read and Brown, 1981). Within the fault zone, ductile fabrics with E-side-down kinematics (Brown and Murphy, 1981; Read and Brown, 1981; Lane et al., 1989) are overprinted by late brittle normal and strike-slip faulting (Lane, 1984). In the northern Thor-Odin culmination, shear bands identical to those found in the Thor-Odin detachment are E-dipping. To distinguish between the ductile and brittle fabrics, we restrict the term "Columbia River fault" to the

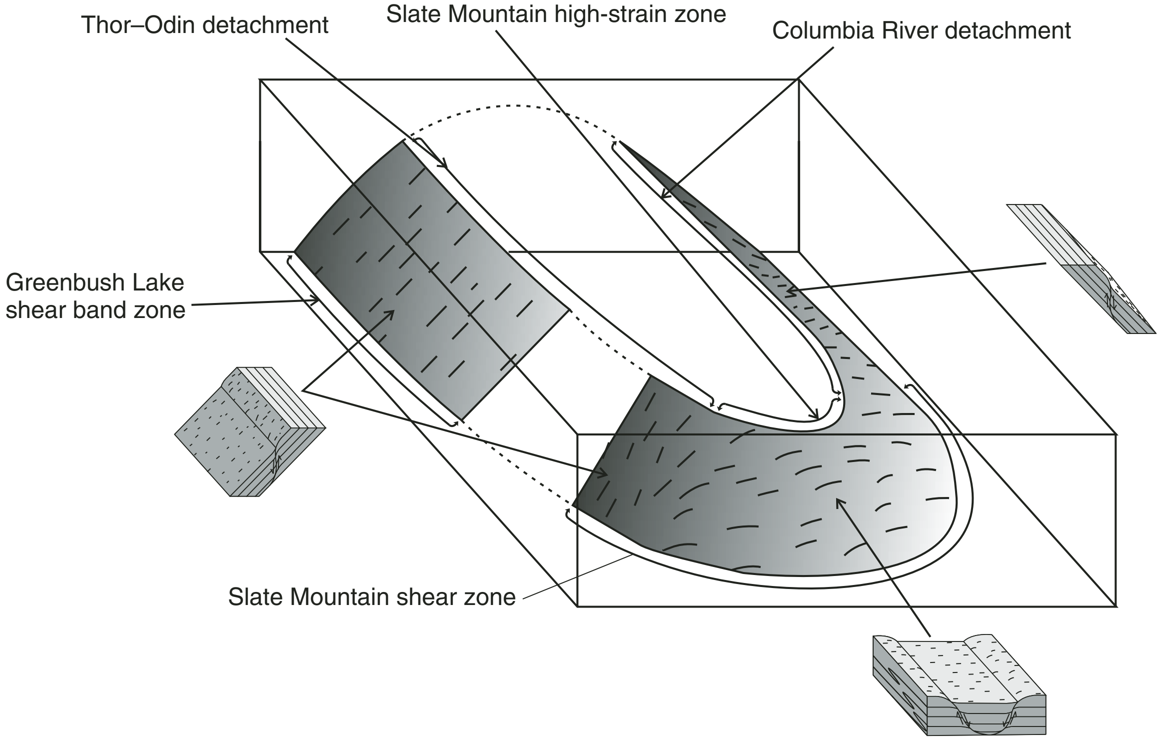

Figure 4. Relationship between the Thor-Odin detachment, Slate Mountain high-strain zone, and Columbia River detachment, collectively referred to as the Thor-Odin high-strain zone. The Thor-Odin detachment is a zone with a diffuse boundary, and it is characterized by down-to-the-W reactivation of the S_T foliation, a downdip sillimanite lineation, and shear bands (C′) consistent with overall W-side-down displacement. The central Slate Mountain high-strain zone is characterized by a horizontal sillimanite lineation and conjugate shear bands that intersect in the foliation plane and are normal to the sillimanite lineation. These observations together are interpreted as being the result of E-W coaxial extension. The Columbia River detachment (ductile Columbia River fault) is characterized by E-side-down shear bands (C′), a downdip lineation, and mylonitic fabrics (Brown and Murphy, 1981; Read and Brown, 1981; Lane et al., 1989).

late brittle overprint, which extends beyond the boundaries of the Monashee complex (Read and Brown, 1981; Lane, 1984). The older, ductile E-side-down high-strain zone, previously interpreted as the Monashee décollement (Brown and Murphy, 1981; Read and Brown, 1981; Brown et al., 1986; Lane et al., 1989; Brown et al., 1992), is interpreted here as the continuation of the Thor-Odin high-strain zone (Fig. 4), and is referred to as the Columbia River detachment. It incorporates the east end of the old Slate Mountain shear zone. Lane et al. (1989) observed overprinting down-to-the-east ductile fabrics in the Columbia River valley, which they interpreted as related to thrust displacement on the Monashee décollement. They concede, however, that these fabrics may also be the result of Eocene ductile extension.

The Thor-Odin detachment is not a sharply defined zone. It does not obviously cut across S_T, but rather, reactivates it. The reactivation may be manifested as a ductile shear parallel to S_T, or it may occur as discrete slip on S_T surfaces (Fig. 5A). There is commonly a well-developed sillimanite lineation on S_T, within the zone, which plunges downdip in a westerly direction (Fig. 5B). Outside the zone, there is a sillimanite lineation on S_T that generally plunges approximately SW. It differs from the sillimanite lineation within the zone, not only in orientation, but also in that it commonly is composed of sillimanite after large (centimeter-scale) prismatic kyanite, with kyanite preserved locally (Fig. 5C). The boundary of the zone is diffuse. Alternating, foliation-parallel, millimeter- to decimeter-wide domains exhibit either the SW-plunging sillimanite after kyanite lineation, a foliation-parallel random sillimanite fabric, or a sillimanite lineation oriented somewhere between the kyanite lineation and the downdip sillimanite lineation (Fig. 5D). Shear bands and displaced markers (Fig. 5A) consistently indicate normal, W-side-down kinematics overprinting the top-to-the NE S_T fabric.

Fabrics in the Slate Mountain high-strain zone are different from both the Thor-Odin detachment and Columbia River detachment. We recognize the Slate Mountain high-strain zone as a broad, diffuse zone (2–4 km wide) characterized by reactivation and modification of the transposition fabric (S_T). Folds are unusually cylindrical, trend horizontally E-W, and have moderately steep to vertical enveloping surfaces. The late sillimanite lineation on S_T is horizontal and E-W trending (Fig. 6A). There are ubiquitous shear bands, which form a conjugate pair that is symmetrical about the lineation and intersects in an axis that lies within the foliation plane (Fig. 6B). This symmetrical relationship indicates that deformation in this part of the Thor-Odin high-strain zone was coaxial with E-W–directed stretching. Along strike toward the east, the sillimanite lineation becomes progressively more E-plunging, and shear bands indicate E-side-down noncoaxial deformation.

The Slate Mountain high-strain zone is kinematically linked to the two normal shear zones (Thor-Odin detachment and Columbia River detachment). It represents a zone of coaxial extension, which commonly develops at the intersection of opposing shear zones (Fig. 7). The overall kinematics of the Thor-Odin high-strain zone indicate movement of material from above the culmination toward its flanks.

Timing constraints on the various segments of the Thor-Odin high-strain zone are incomplete

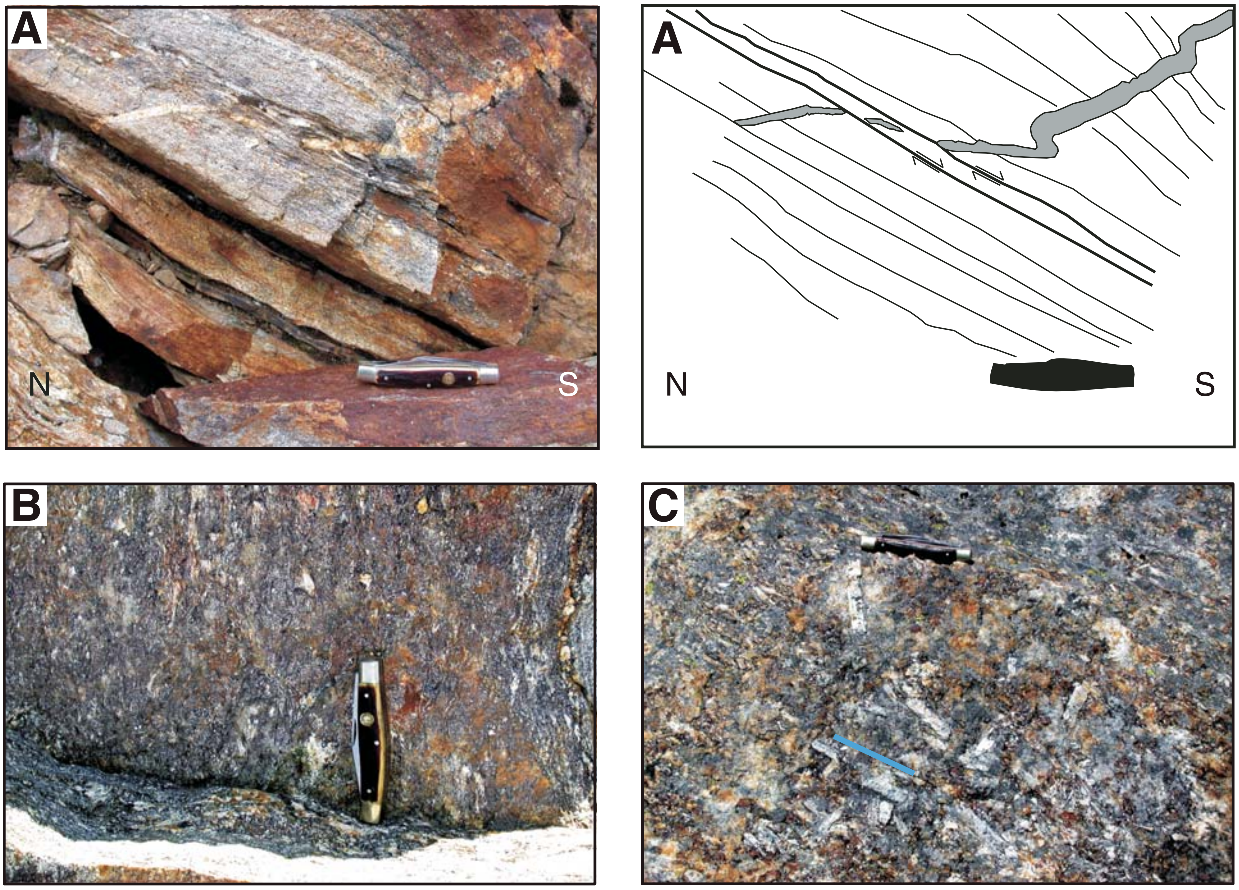

Figure 5. Kinematics of the Thor-Odin detachment. Pen knife (~10 cm) is for scale. (A) Photograph and line drawing of pegmatite dike crosscutting the S_T foliation. Vergence of folds in pegmatite is consistent with early top-to-the-NE noncoaxial flow (transposition). This pegmatite was subsequently deformed by SW-side-down reactivation of the transposition foliation (S_T). (B) Downdip sillimanite lineation characteristic of a foliation surface reactivated by the normal shear. (C) S_T transposition fabric plane just outside the shear zone unaffected by extensional reactivation. Kyanite grains (partially altered to sillimanite) in the foliation are lineated toward the SW (blue line). (D) Same outcrop as in C. Reactivated foliation surface is parallel to, but separated from, the surface shown in C by 2 cm. Lineation is defined by sillimanite (red line) with an orientation intermediate between the downdip lineation in B and the SW-pitching lineation in C (blue line). Pen knife for scale is outlined in yellow.

Figure 6. Fabrics from the coaxially deformed Slate Mountain high-strain zone. Compass (~10 cm) is for scale. (A) Horizontal sillimanite lineation on the stretched S_T surface, consistent with E-W coaxial extension. (B) Photograph and line drawing of the same outcrop perpendicular to S_T containing symmetrical boudins and minor conjugate shear bands. The intersection defined by the conjugate shear bands is orthogonal to the horizontal sillimanite lineation and lies within S_T.

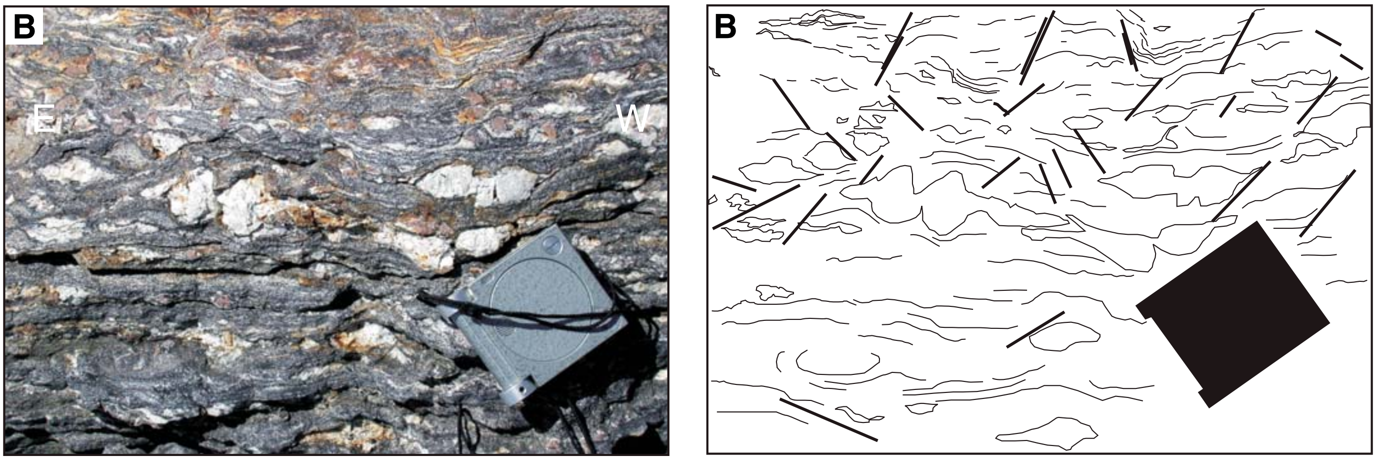

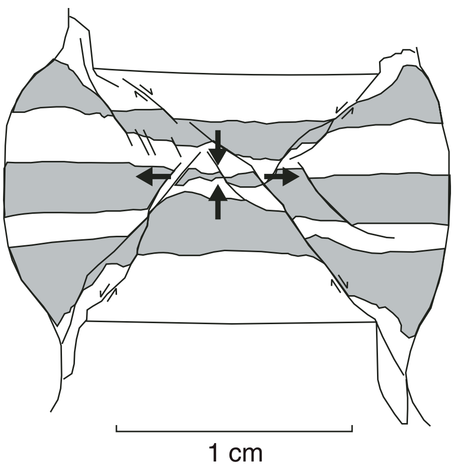

Figure 7. Experimentally produced shear bands (modified from Means and Williams, 1972). The layers in this specimen were originally of constant thickness, and their boundaries are planar and parallel. Imposed layer-parallel extension (160%) is accommodated by conjugate, noncoaxial shear. At the crossover zone between conjugate shears bands, a zone of coaxial thinning has developed.

but consistent with coeval Eocene extension. Johnston et al. (2000) reported shear bands from the Greenbush Lake shear band zone that are cut by 50.2 ± 0.5 Ma (monazite U-Pb age) pegmatite dikes. Parrish et al. (1988) suggested that top-to-the-E mylonites are also early Eocene in age. Lane et al. (1989) stated that ductile top-to-the-E mylonites could either be related to Late Cretaceous to Paleocene thrust movement on the Monashee décollement, or to Eocene normal displacement on the Columbia River fault (Columbia River detachment in this contribution). No geochronological data are available for the age of the Slate mountain shear zone, but Carr (1991) suggested that fabrics within the Slate Mountain shear zone are similar to ductile fabrics in Eocene normal shear zones elsewhere in the region. Further geochronological work would provide a valuable test of the correlations proposed here.

Seismic Data

Profile 6 and merged profile 7–8–9 (Fig. 1) were recorded south of the Thor-Odin culmination (Cook et al., 1988, 1992). Acquisition and processing parameters are described in Cook et al. (1988, 1992). True 3-D seismic data were collected and interpreted in a restricted area at the intersection of lines 6 and 7–8–9 (Vasudevan et al., 1995). The 3-D data show a SW-dipping reflection consistent with the projections of the Monashee reflection developed here; however, the interpreted area is too restricted to test for possible surface correlations.

All of the seismic profiles are characterized by a penetrative, parallel, and curvilinear seismic-reflection fabric (Fig. 2A), which is consistent in appearance and orientation with the transposition fabric (S_T) seen on the present topographic surface. On profile 6, the Monashee reflection is a clear discontinuity, the trace of which plunges south at ~24°S (Fig. 2B). The Valhalla reflection discontinuity occurs only in the hanging wall of the Monashee reflection (Fig. 8). The Valhalla reflection is curved and truncates penetrative fabric below but appears approximately parallel to the fabric above. Curvature of the latter is consistent with east-west–trending kilometer-scale folds known throughout the Thor-Odin culmination and in the region to the south (Carr, 1991). The trace of the Valhalla reflection ends

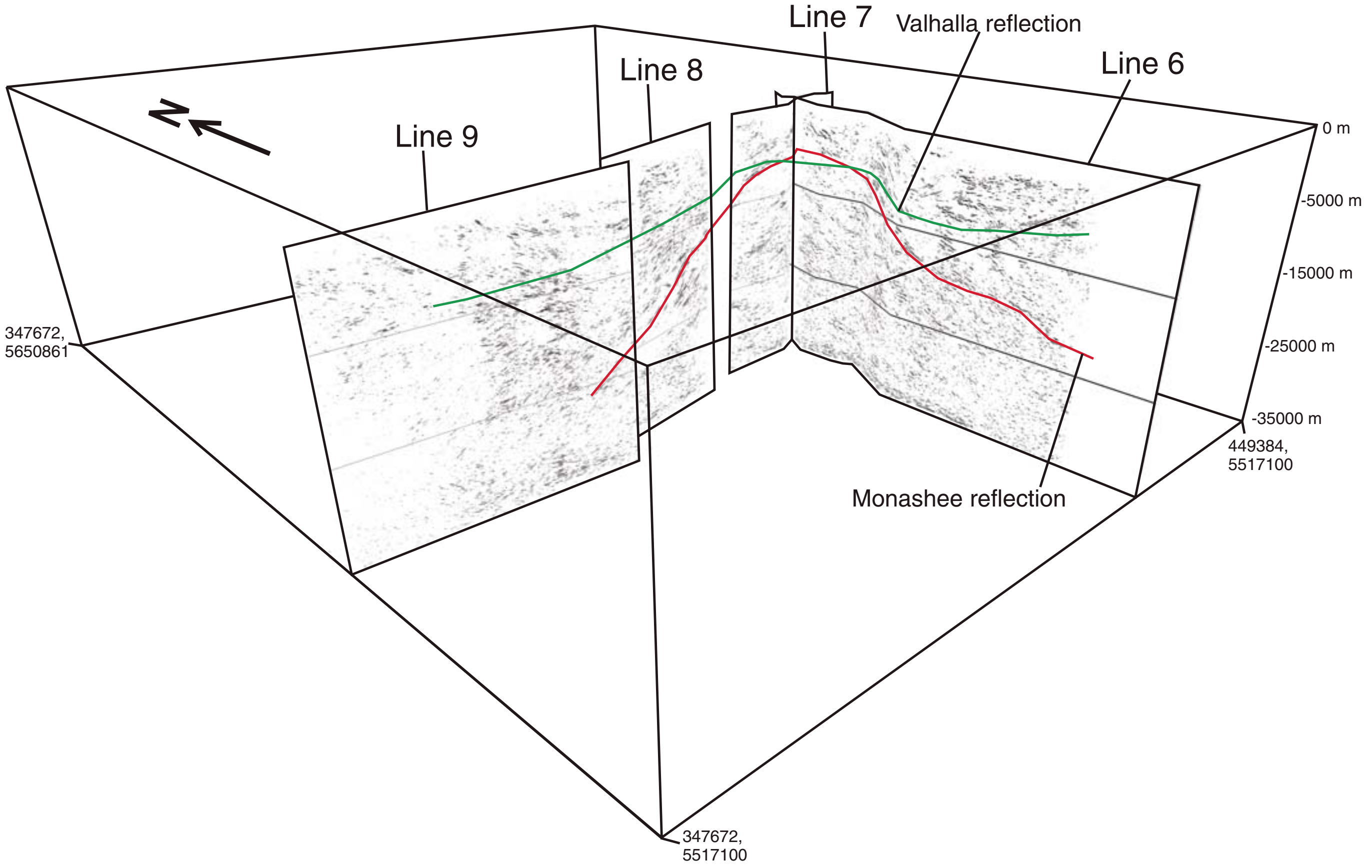

Figure 8. Relationship between the Valhalla reflection (VR, green trace) and Monashee reflection (MR, red trace). The Valhalla reflection is truncated by the Monashee reflection and does not appear on the seismic section in the footwall of the Monashee reflection. Horizontal coordinates are in UTM, and vertical axis is in meters.

at the Monashee reflection and has previously been interpreted to merge with the Monashee reflection (Carr, 1995). Geometrically, however, this relationship is equally consistent with truncation of the Valhalla reflection by the Monashee reflection if the Valhalla reflection is now above ground level on the footwall side of the Monashee reflection.

On profile 7–8–9 (Fig. 2), the trace of the Monashee reflection plunges ~27°W at the west end of the profile. The Monashee reflection is clearly curved, and its trace changes from W-plunging to shallowly E-plunging (20°) near the eastern end of the profile. The penetrative seismic fabric in the hanging wall curves into the discontinuity and has a concave upward sense of curvature. In the footwall, the presence of concave-up reflections, which are considered to be a processing artifact (Cook et al., 1992) near the gap between profiles 7 and 8, makes interpretation difficult. It appears, however, that the Monashee reflection is both parallel to and crosscutting with respect to footwall reflections in different locations. There is a poorly defined second discontinuity in the hanging wall of the Monashee reflection at a similar level to the Valhalla reflection on profile 6. This discontinuity is curved and cuts across the underlying penetrative fabric, but it appears approximately parallel to the overlying penetrative fabric. We interpret it as the trace of the Valhalla reflection (Fig. 8).

The Bevan and Cherryville faults are known from surface mapping, but they do not appear as reflections on the seismic profiles (Fig. 2B). Interpretation of these structures is unchanged from existing published interpretations (cf. Cook et al., 1988; Carr, 1991; Brown et al., 1992; Cook et al., 1992).

Surface Projections and Correlations

Central to the arguments concerning the origin of the Monashee reflection is the correlation of the Monashee reflection with surface features. Based on different sets of geometric assumptions, three 3-D structural models of the Monashee reflection (Fig. 3) were constructed using commercially available software (FLEDERMAUS by IVS Inc.).

The seismic profiles were projected as georeferenced vertical panels. Since the Lithoprobe acquisition lines made use of crooked mountain roads, treating profiles as planes introduced apparent dip errors. Major bends in the acquisition line were honored in the projection to correct for this as much as possible. X, Y, and Z points on the Monashee reflection were then manually selected and contoured. Digital elevation models (DEMs) were generated from the structure contours and intersected with a digital terrain model (DTM) of the southern Thor-Odin region. The Thor-Odin DTM is based on 1:20,000 British Columbia Terrain Resource Information Mapping (BC-TRIM) data and is draped with a recent geological compilation map (Kruse et al., 2004).

The accuracy of these 3-D projections is unavoidably constrained by geophysical sources of error, including depth-time relationship, out-of-profile dipping structures, and choice of datum, all of which can lead to error in the apparent dip of reflections in their respective profiles. A detailed analysis of the velocity structure of the crust would improve the precision of the projections, but not necessarily the accuracy, due to the inherent geometric assumptions.

Model 1 (Animation 1) is a construction based on purely geometrical interpretation of the seismic reflections, and it incorporates no geological knowledge or interpretation. The straightness of the Monashee reflection on profile 6 (Fig. 2B) and curvature above 6 s on profile 7–8–9 are consistent with a S-plunging cylindrically folded surface (Hobbs et al., 1976), with the axis parallel to the trend of profile 6. Assuming cylindricity, structure contours were generated by projecting down- and up-plunge from the trace of the reflection onto horizontal surfaces representing different relative levels above and below the present topographic surface (Fig. 9A). Below 6 s, the apparent dip of the reflection becomes progressively shallower as it approaches the Moho at 12 s, and the plunging cylindrical surface model no longer approximates the reflection.

Model 2 (Animation 2) also assumes a plunging cylindrical surface, but with an axis trending parallel to the overall elongation direction of the Monashee complex (340°, Fig. 9B). This interpretation is not necessarily in conflict with the straight-line trace of the Monashee reflection above 6 s on section 6. The radius of curvature of the southern end of the culmination is large, and the difference between this plunge direction and that assumed for model 1 is fairly small (28°). Thus, the trace of the new surface above 6 s on section 6 can still approximate a straight line within the limit of detection.

Model 3 (Animation 3) is a forced fit of the reflection to the southern Thor-Odin detachment and the Slate Mountain high-strain zone (Fig. 9C). Data do not extend far enough to include the Columbia River detachment. A triangulated irregular network (TIN) was constructed using manually selected X, Y, and Z points on the traces of the reflections and on the surface position of the high-strain zone. Intermediate points were linearly interpolated on the surface of the TIN. Because the model assumes a correlation and interpolates a surface, it has no predictive value. Model 3, however, is useful for testing such a correlation for geological veracity. A weakness of this technique is that equal weight is given to geological or geophysical noise, such as perturbations on the surface caused by minor (at the scale of a crustal-scale profile) faults, folds, reflections from igneous bodies, or processing artifacts. Statistical surface fitting techniques, such as regression or moment-of-inertia analysis, are a poor choice in this case because data points on the seismic sections are nearly collinear (Fernández, 2005).

All three surfaces mimic the mapped geology of the Thor-Odin culmination in that they indicate southerly plunging antiformal structures (Fig. 10). However, they vary considerably in detail. The model 1 trace closes too far south and cuts markedly across S_T in the southwest. It is close in orientation and position to the Thor-Odin high-strain zone along the western flank of the culmination (Fig. 10). The model 2 surface is the poorest fit. It closes too far north and west of the mapped closure and cuts across S_T everywhere (Fig. 10). Since it is so constructed, the model 3 surface trace fits the Thor-Odin high-strain zone well, except where smoothing of the surface, inherent in DEM construction, causes minor deviation (Fig. 10). Its angular appearance, due to the linear interpolation of data points between the two profiles during construction of the TIN, is not consistent in style with the observed curvature of the Thor-Odin culmination. The model can be smoothed (Fig. 9D) to produce a realistic periclinal structure that is consistent with the observed structure of Thor-Odin (a periclinal culmination) and honors all surface (trace of Thor-Odin high-strain zone) and subsurface (Monashee reflection) data points. The main difference between model 1 and the smoothed model 3 is that model 1 is cylindrical, whereas the plunge of model 3 decreases gently to the north. Thus, the Thor-Odin high-strain zone and Monashee reflection can be joined by a structure that is geologically reasonable and reflects the overall geometry of the Thor-Odin culmination and is consistent with the interpretation of the Monashee reflection as a normal structure overprinting the transitional zone between the transposed basement and middle-crustal zone.

Evidence for Normal Displacement

Geometry of the Monashee Reflection

The geometry of the reflection and its hanging wall and footwall are consistent with a normal shear zone rather than a thrust ramp. If the hanging wall had been displaced to the northeast over a thrust ramp (Brown et al., 1992; Cook et al., 1992; McNicoll and Brown, 1995; Varsek and Cook, 1994; Carr, 1995), the reflections above the ramp should all be parallel to it (Fig. 11A). Instead, the hanging-wall reflectors are nearly flat-lying except very near to the Monashee reflection, where they curve progressively into the discontinuity, analogous to a down-to-the-SW shear band (Fig. 12). In addition, reflections in the hanging wall are convergent (Fig. 2B) toward the crest of the Monashee reflection on line 7–8–9, suggesting an attenuated zone over the top of the footwall block analogous to the thinned zone over the crest of a boudin (cf. Davis and Coney, 1979; Jolivet et al., 2004) and consistent with the shear sense variation in the Thor-Odin high-strain zone.

Metamorphic Pressures

Recorded pressures west of the Thor-Odin detachment are lower than those to the east of it, which is consistent with normal displacement of isograds (Fig. 11B). Pressure estimates from amphibolite boudins in the Selkirk allochthon (Three Valley Gap assemblage, immediately west of Thor-Odin) are 6–7 kbar (Ghent et al., 1977). In the southern Thor-Odin culmination, Norlander et al. (2002) reported maximum metamorphic pressures of 8–10 kbar. Metamorphic pressures should increase toward the footwall in extensional-detachment–type core complexes and decrease toward the footwall in thrust-type culminations (Yin, 2004) (Fig. 11).

The Monashee reflection is traceable on line 7–8–9 as a discrete surface to a depth of 10 s or ~30 km (Fig. 2B). In the Monashee décollement interpretation (see Brown et al., 1986, and references therein), the Monashee reflection represents a ductile thrust ramp that places middle- and upper-crustal rocks (Selkirk allochthon) on top of the Monashee complex rocks with 80–100 km of transport. To be consistent with the seismic section, the base of the Selkirk allochthon must have come from a depth of ~25 km greater than the crest of the Monashee complex. Given this situation, it is to be expected that the highest pressures recorded in the Selkirk allochthon would be significantly higher than the highest pressures in the Monashee complex.

If the Monashee décollement was initially a thrust flat, or a lower-amplitude ramp that was arched during late extension (see Brown et al., 1992, and references therein), then pressures across the surface expression of the Monashee reflection could be the same. Neither version of the Monashee décollement model addresses why metamorphic pressures in the Selkirk allochthon are lower. In addition, if the Monashee reflection had been significantly arched late in its evolution, then it would require that the now approximately horizontal reflection fabric (Fig. 2A) below the Monashee reflection was originally concave upward, and would also require considerable relief on the Moho, which has subsequently been removed.

Geochronological Argument

The Monashee complex and surrounding area are characterized by a younging of peak metamorphic and deformational ages with increasing structural depth (see Carr, 1991; Carr, 1995; Parrish, 1995; Gibson et al., 1999; Crowley et al., 2001; Johnston et al., 2000; Kuiper et al.,

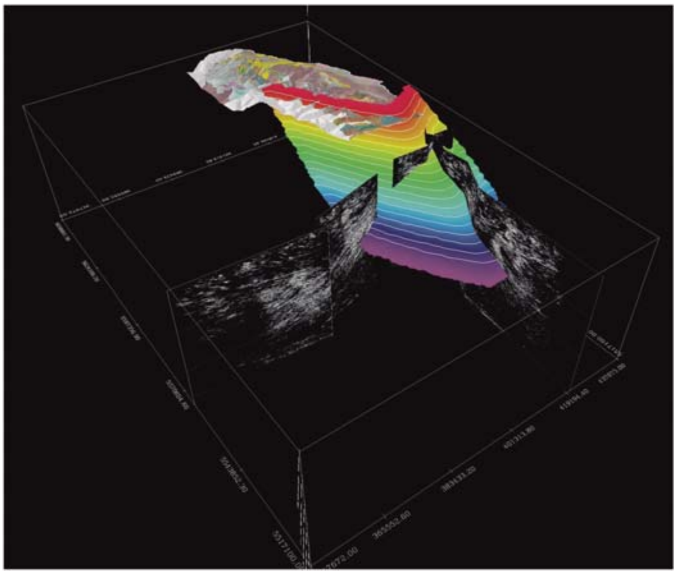

Animation 1. Monashee reflection model 1: Cylindrical plunging surface with an axis parallel to section 6 (plunging 24° toward 188°). Surface trace roughly coincides with the shape of the Thor-Odin high-strain zone but is offset geographically. Lithoprobe seismic profiles 6 and 7–8–9 are projected as bent surfaces to honor major bends in the acquisitions lines. The surface compilation map (Kruse et al., 2004) is draped over a digital terrain model (DTM created from 1:20,000 British Columbia Terrain Resource Information Management Program topography data). The digital elevation models of the Monashee reflection are projected up-plunge to intersect the surface geology. If you are viewing the PDF, or if you are reading this offline, please visit http://dx.doi.org/10.1130/GES00049.S1 to view the animation.

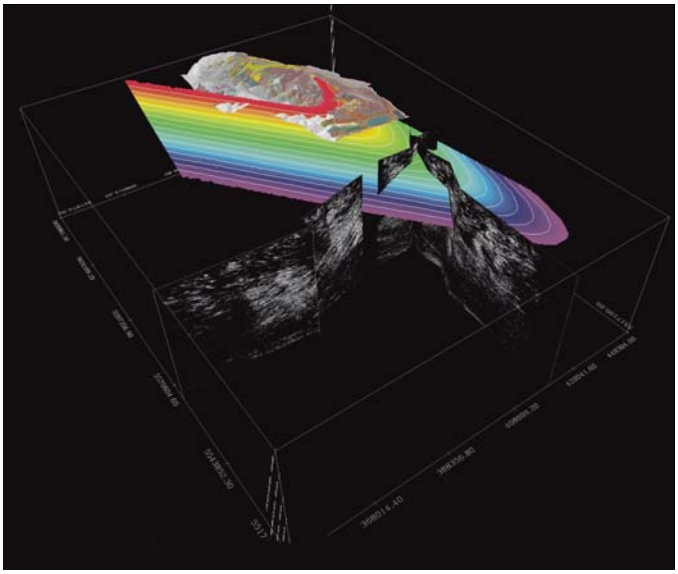

Animation 2. Monashee reflection model 2: Cylindrical plunging surface with an axis parallel to the trend of the Monashee complex (plunging 13° toward 160°). Surface trace of the Monashee reflection cuts across regional fabric (S_T). Lithoprobe seismic profiles 6 and 7–8–9 are projected as bent surfaces to honor major bends in the acquisitions lines. The surface compilation map (Kruse et al., 2004) is draped over a digital terrain model (DTM created from 1:20,000 British Columbia Terrain Resource Information Management Program topography data). The digital elevation models of the Monashee reflection are projected up-plunge to intersect the surface geology. If you are viewing the PDF, or if you are reading this offline, please visit http://dx.doi.org/10.1130/GES00049.S2 to view the animation.

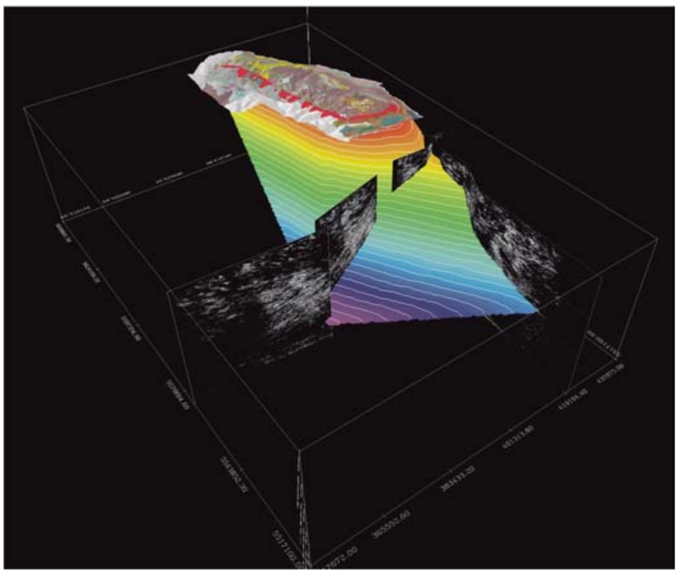

Animation 3. Monashee reflection model 3: Triangulate irregular network (TIN) digital elevation model (DEM) of an arbitrary surface containing the two seismic traces of the Monashee reflection and the surface trace of the southwestern portion of the Thor-Odin high-strain zone (TOHZ). The overall surface is slightly angular, and there is no single well-defined axis due to the linear interpolation between data points. Lithoprobe seismic profiles 6 and 7–8–9 are projected as bent surfaces to honor major bends in the acquisitions lines. The surface compilation map (Kruse et al., 2004) is draped over a digital terrain model (DTM created from 1:20,000 British Columbia Terrain Resource Information Management Program topography data). If you are viewing the PDF, or if you are reading this offline, please visit http://dx.doi.org/10.1130/GES00049.S3 to view the animation.

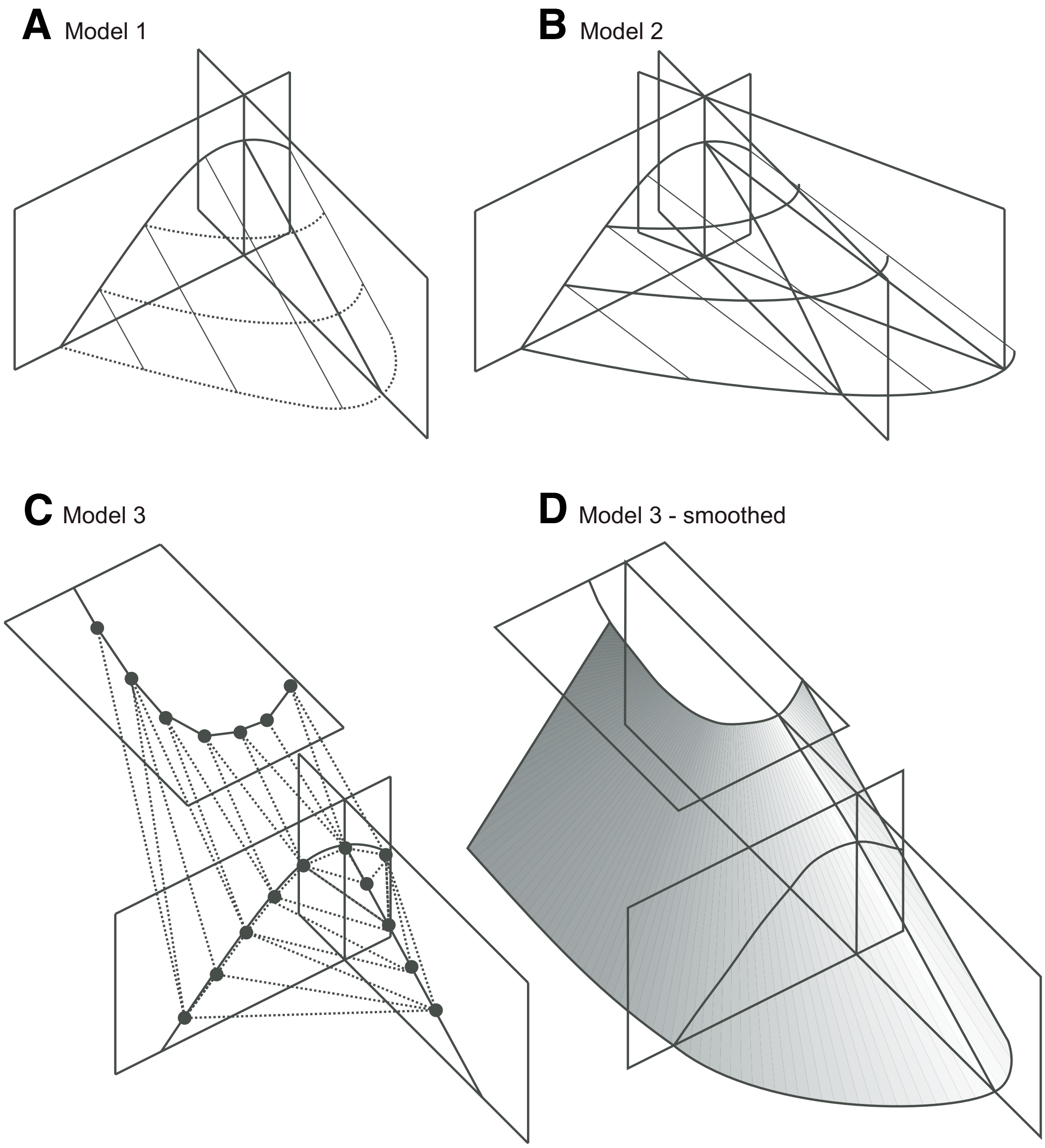

Figure 9. Projection method. Seismic-profile planes are illustrated as planar for the sake of clarity. In actuality, the lines have been projected as a series of vertical planes closely approximating the sinuous transect line. (A) Model 1: The relative straightness of the trace of the Monashee reflection above 21 km (7 s) suggests that the trend of section 6 is close to the trend of the axis of curvature of a cylindrical, plunging surface. Projecting this axis of curvature to a horizontal datum produced a contour that can be interpolated at any position on the trace of the reflection. (B) Model 2: Similar to model 1, but the axis of curvature is assumed to trend parallel to the overall trend of the Monashee complex (160°). (C) Model 3: A triangulate irregular network (TIN) digital elevation model (DEM) of an arbitrary surface containing the two seismic traces of the Monashee reflection and the surface trace of the Thor-Odin high-strain zone. (D) Realistically smoothed, periclinal version of model 3 that joins the seismic traces of the Monashee reflection and the surface trace of the Thor-Odin high-strain zone.

2006). Johnston et al. (2000) and Kuiper (2003) documented a hiatus in the U-Pb age of F_3 folds across the Thor-Odin detachment. To the west, on Joss Mountain, F_3 folds are Late Cretaceous in age, whereas at Blanket Mountain, east of the Thor-Odin detachment, F_3 folds are Eocene in age (Johnston, 1998; Johnston et al., 2000; Kuiper, 2003). This hiatus is consistent with normal offset of a downward-younging strain pattern (Fig. 11), but it is not consistent with thrusting.

Regional Extension

Regionally the southern Omineca belt is characterized by Mesozoic to early Eocene contractional structures overprinted by Eocene extensional structures (Brown and Journeay, 1987; Parrish et al., 1988; Johnston et al., 2000; Kruse and Williams, 2005; Williams and Jiang, 2005). The Monashee reflection crosscuts reflections, which appear to represent the transposition foliation and large-scale folds. The observation that the Monashee reflection appears to crosscut all earlier structures and fabrics is consistent with extensional structures throughout the region.

Mesoscopic shear bands are ubiquitous in the Thor-Odin culmination, and like the Monashee reflection, individual shear bands may simply deflect the pre-existing foliation in one place while truncating it elsewhere (compare Figs. 2A and 12). The shear bands are self-similar structures, and they occur at all scales, from microscopic to fully exposed examples with strike lengths of several kilometers. Based on the principle of self-similarity of structures (Pumpelly et al., 1894; Turner and Weiss, 1963, p. 188; Hobbs et al., 1976, p. 368), it is reasonable to expect orogen-scale shear bands as well.

DISCUSSION

The Monashee reflection is one of the largest and most prominent reflections recorded by the Lithoprobe program in the southern Cordillera. As such, it could be argued that it must have a large displacement. However, analogous to mesoscopic shear bands (Fig. 12), the displacement need not be large in order to deflect the foliation in the host rock into flanking fault-drag folds (Means and Williams, 1972). In addition, the maximum pressure difference between the Monashee complex basement and middle-crustal zone rocks (1–4 kbar, corresponding to a throw of 3.1–15.4 km) suggests that displacement,

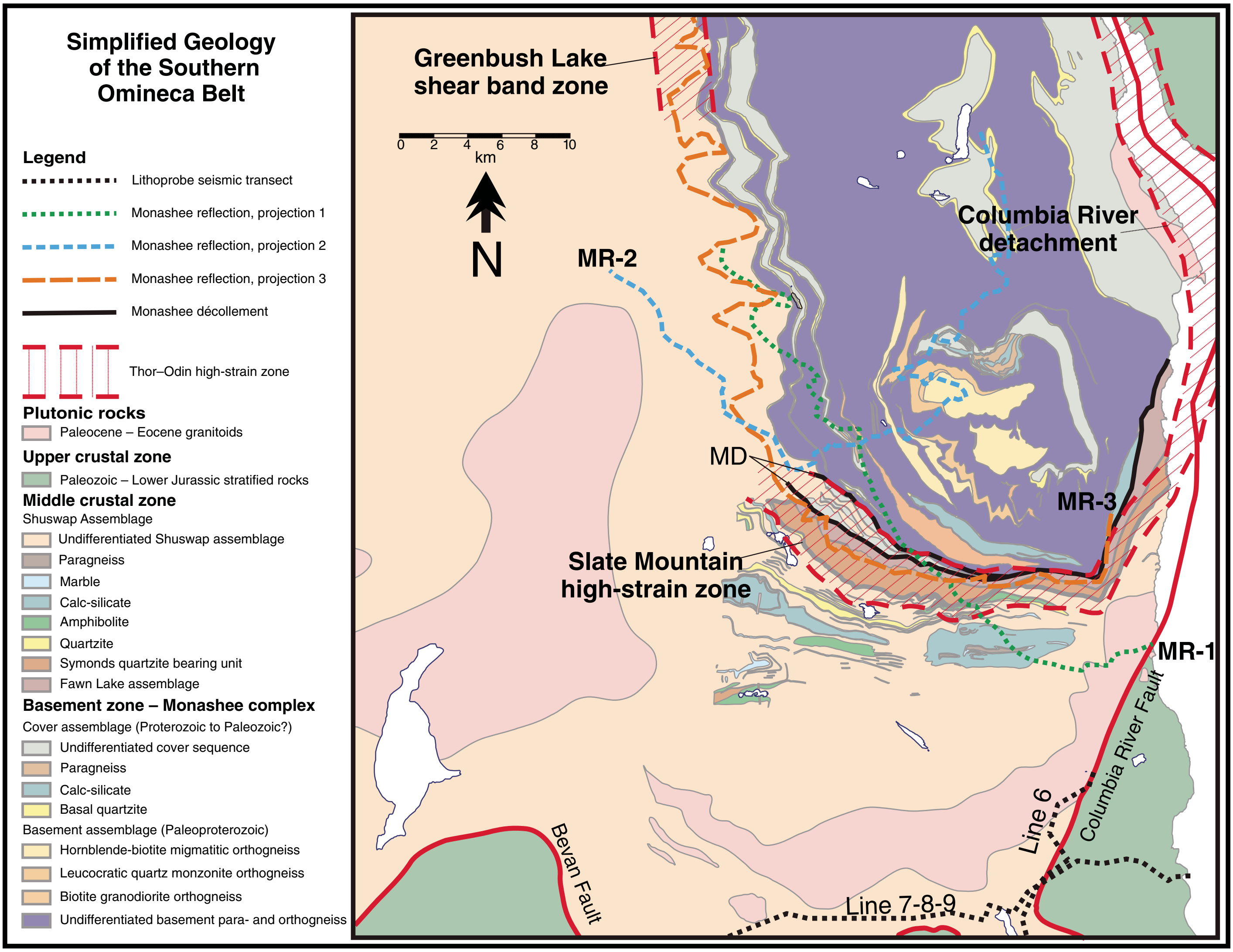

Figure 10. Geology of the southern Thor-Odin and Pinnacles area (Kruse et al., 2004) and the projected surface trace of the Monashee reflection according to models 1, 2, and 3 (MR-1, MR-2, and MR-3, respectively), along with the locations of the Monashee décollement (MD) according to McNicoll and Brown (1995), Slate Mountain shear zone (Carr, 1991), Slate Mountain high-strain zone, and Greenbush Lake shear band zone (Johnston, 1998; Johnston et al., 2000).

and thus shear strain on the Thor-Odin detachment, is relatively low (γ = 3.12–15.3), assuming a mean dip of 30°, simple shear, and a true thickness of 2 km. This is consistent with qualitative estimates of the strain in the Greenbush Lake shear band zone. Mesoscopic shear bands (Fig. 12) with clear offset markers record shear strains of γ = 3.8–20, with a mean of γ = 9.8, within the same order of magnitude as estimated for the Monashee reflection from the surface-pressure differential. The estimation of displacement is complicated by several late brittle faults that outcrop close to the Thor-Odin detachment and have a similar strike. They are interpreted as transcurrent faults, but they generally appear to have been reactivated by W-side-down displacement. In the northern Thor-Odin culmination, one such fault, the Victor Creek fault, has minimum displacement of at least 1.3 km (Kruse and Williams, 2005). The exact displacement vector is unknown, but considerable dip-slip displacement on the Victor Creek fault is possible. Thus, a component of the offset of the pressure gradient could be due to late brittle displacement. The minimum displacement is also constrained by the absence of a Valhalla reflection footwall trace. A normal throw of ~6 km would place the Valhalla reflection above the current level of erosion (Fig. 8). Thus, a final estimate of throw on the Monashee reflection is 6–15 km (discounting the effect of brittle faults), although the similar structural style and lithological units on either side of the Greenbush Lake Thor-Odin detachment suggest that the displacement is closer to the minimum value.

An alternative hypothesis is that the Monashee reflection represents the base of Cordilleran deformation, below which only Proterozoic fabrics are observed. If this is the case, then the Monashee reflection must be exposed only in Frenchman Cap, where the base of Cordilleran deformation has been reported (Crowley et al., 2001; Gervais et al., 2005). This requires a much more rapid flattening of the plunge of the Monashee reflection than is suggested by the projection models (Animations 1–3) and does not account for the Thor-Odin high-strain zone observed around the margins of Thor-Odin.

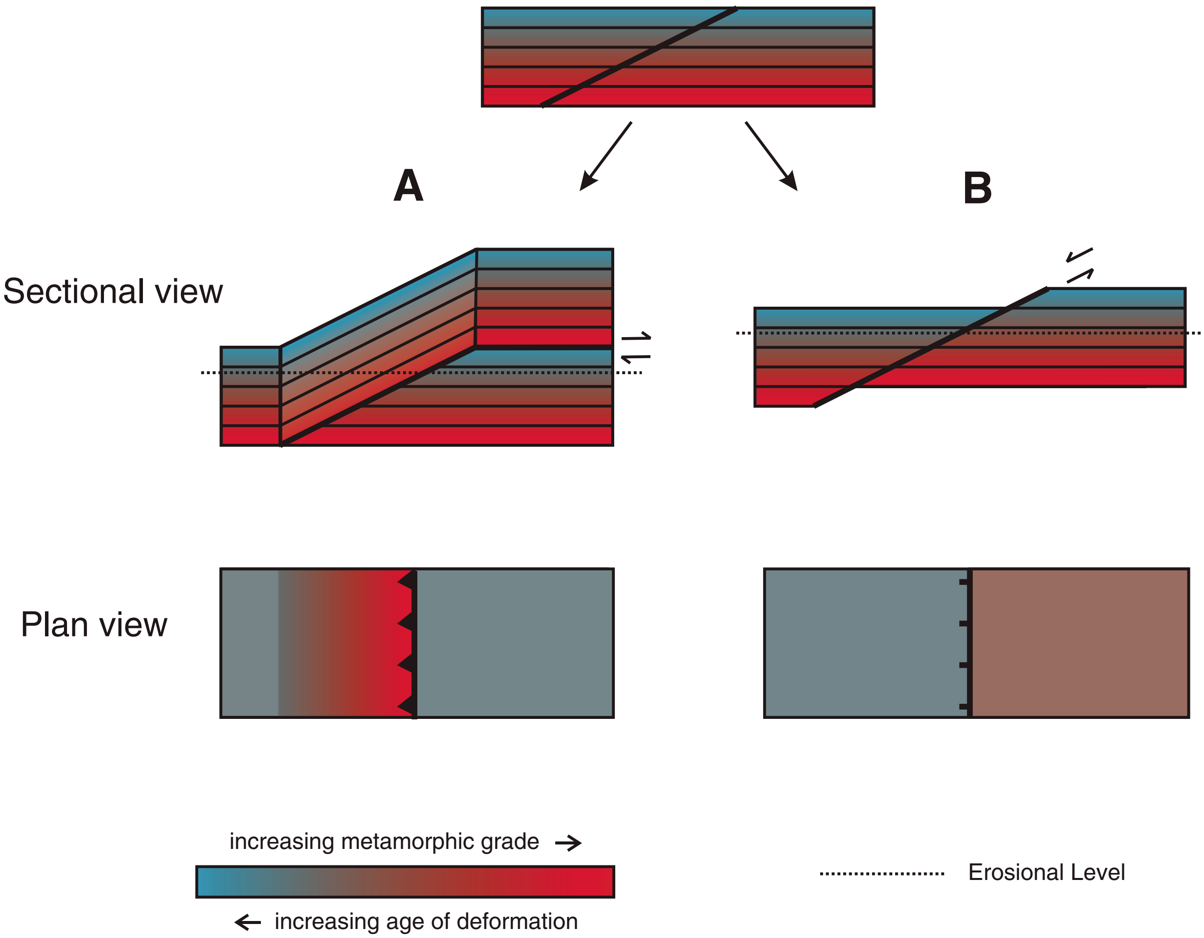

Figure 11. Geometric consequences of thrust fault (A) versus a normal shear zone (B) interpretation of the Monashee reflection. Note that in the thrust ramp interpretation of the Monashee reflection, the fabric above the thrust ramp is parallel to the detachment surface. Compare this geometry with the seismic sections in Figure 2. (A) Offset of prefaulting geochronological and metamorphic gradients along a thrust fault produces older ages and lower grades in the footwall block. (B) Offset of prefaulting geochronological and metamorphic gradients along a normal fault produces younger ages and higher metamorphic grades in the footwall block.

Figure 12. Quartzite hand specimen containing a shear band from the northern Thor-Odin culmination. Note that the overall displacement is not great, but it is sufficient to deflect the surrounding foliation into flanking fault-drag folds. Analogous with the seismic section, some layers are truncated while others curve gradually into the shear band.

Another alternative interpretation of the Monashee reflection is that it is a Proterozoic structure that predates and is below the level of Mesozoic Cordilleran deformation (Thompson et al., 2002). There are no known candidates for this kind of structure at the surface; thus, this hypothesis requires that the Monashee reflection not outcrop at all. In addition, given that the crust in the southern Cordillera thins from 45 to 36 km, east to west (Cook, 1995a), it is unclear how this crustal thinning could be accommodated without affecting structures below ~6 km depth, unless the thinning occurred during the Proterozoic as well (Cook, 1995b).

CONCLUSIONS

The Monashee reflection is a major crustal-scale, crosscutting reflection that appears on Lithoprobe seismic profiles. It is interpreted as the subsurface representation of the Thor-Odin high-strain zone, which incorporates previously reported structures, including the Greenbush Lake shear band zone, Slate Mountain shear zone, and the ductile Columbia River fault. Kinematics of the Thor-Odin high-strain zone are consistent with E-W stretching or vertical movement of the complex resulting in transport of material away from the crest of the culmination toward its flanks.

A normal shear sense on the Monashee reflection is supported by: (1) the probable correlation of the Monashee reflection with the Thor-Odin high-strain zone; (2) the fault-drag–like deflection of reflections into the Monashee reflection and the convergence of reflections over the crest of the Monashee reflection; (3) higher peak metamorphic pressures in the Monashee complex than in the surrounding middle-crustal zone rocks; and (4) a hiatus in the age of deformation across the Thor-Odin high-strain zone.

Pressure differences across the zone and the absence of the Valhalla reflection in the footwall of the Monashee reflection provide an estimate of throw on the Monashee reflection of 6–15 km. Similarity of lithological units and structural style across the Thor-Odin detachment leads us to favor a true displacement closer to the minimum constraint.

ACKNOWLEDGMENTS

Thanks are extended to Arie J. van der Velden and Fred A. Cook for introducing us to the Lithoprobe data and for many subsequent discussions. Paul McNeill and Andy Parmenter are thanked for their input on the geology of the Thor-Odin culmination. We thank reviewers Mike Williams, Dan Gibson, and John Hole. The work was supported by a Natural Sciences and Engineering Research Council Discovery Grant awarded to Williams.

REFERENCES CITED

Armstrong, R.L., 1982, Cordilleran metamorphic core complexes—From Arizona to southern Canada: Annual Review of Earth and Planetary Sciences, v. 10, p. 129–154, doi: 10.1146/annurev.ea.10.050182.001021.

Armstrong, R.L., Parrish, R.R., van der Heyden, P., Scott, K., and Runkle, D., 1991, Early Proterozoic basement exposures in the southern Canadian Cordillera: Core gneiss of Frenchman Cap, Unit I of the Grand Forks Gneiss, and Vaseaux Formation: Canadian Journal of Earth Sciences, v. 28, p. 1169–1201.

Bardoux, M., and Mareschal, J.-C., 1994, Extension in south-central British Columbia: Mechanical and thermal controls: Tectonophysics, v. 238, p. 451–470, doi: 10.1016/0040–1951(94)90068-X.

Bosdachin, R., and Harrap, R.M., 1988, Stratigraphy and structure of the Monashee complex and overlying rocks adjacent to the Trans-Canada Highway, west of Revelstoke, B.C., *in* Current Research, Part E: Geological Survey of Canada Paper 88-1E, p. 19–23.

Brown, R.L., and Journeay, J.M., 1987, Tectonic denudation of the Shuswap metamorphic terrane of southeastern British Columbia: Geology, v. 15, p. 142–146, doi: 10.1130/0091–7613(1987)15<142:TDOTSM>2.0.CO;2.

Brown, R.L., and Murphy, D.C., 1981, Kinematic interpretation of mylonitic rocks in part of the Columbia River fault zone, Shuswap terrane, British Columbia: Canadian Journal of Earth Sciences, v. 19, p. 456–465.

Brown, R.L., and Read, P.D., 1983, Shuswap terrane of British Columbia: A Mesozoic "core complex": Geology, v. 11, p. 164–168, doi: 10.1130/0091–7613(1983)11<164:STOBCA>2.0.CO;2.

Brown, R.L., Journeay, J.M., Lane, L.S., Murphy, D.C., and Rees, C.J., 1986, Obduction, backfolding, and piggyback thrusting in the metamorphic hinterland of the southeastern Canadian Cordillera: Journal of Structural Geology, v. 8, p. 255–268, doi: 10.1016/0191–8141(86)90047–7.

Brown, R.L., Carr, S.D., Johnson, B.J., Coleman, V.J., Cook, F.A., and Varsek, J.L., 1992, The Monashee décollement of the southern Canadian Cordillera: A crustal-scale shear zone linking the Rocky Mountain foreland belt to lower crust beneath accreted terranes, *in* McClay, K.R., ed., Thrust Tectonics: London, Chapman Hall, p. 357–364.

Carr, S.D., 1991, Three crustal zones in the Thor-Odin–Pinnacles area, southern Omineca belt, British Columbia: Canadian Journal of Earth Sciences, v. 28, p. 2003–2023.

Carr, S.D., 1995, The southern Omineca belt, British Columbia: New perspectives from the Lithoprobe Geoscience Program: Canadian Journal of Earth Sciences, v. 32, p. 1720–1739.

Cook, F.A., 1995a, The reflection Moho beneath the southern Canadian Cordillera: Canadian Journal of Earth Sciences, v. 32, p. 1520–1530.

Cook, F.A., 1995b, Lithospheric processes and products in the southern Canadian Cordillera: A Lithoprobe perspective: Canadian Journal of Earth Sciences, v. 32, p. 1803–1824.

Cook, F.A., Green, A.G., Simony, P.S., Price, R.A., Parrish, R.R., Milkereit, B., Gordy, P.L., Brown, R.L., Coflin, K.C., and Patenaude, C., 1988, Lithoprobe seismic reflection structure of the southeastern Canadian Cordillera: Initial results: Tectonics, v. 7, p. 157–180.

Cook, F.A., Varsek, J.L., Clowes, R.M., Kanasewich, E.R., Spencer, C.S., Parrish, R.R., Brown, R.L., Carr, S.D., Johnson, B.J., and Price, R.A., 1992, Lithoprobe crustal reflection cross section of the southern Canadian Cordillera. 1: Foreland thrust and fold belt to Fraser River fault: Tectonics, v. 11, p. 12–35.

Craig, D.B., 1966, Structure and Petrology within Shuswap Metamorphic Complex Revelstoke, British Columbia [Ph.D. thesis]: Madison, Wisconsin, University of Wisconsin, 130 p.

Crowley, J.L., 1999, U-Pb geochronologic constraints on Paleoproterozoic tectonism in the Monashee complex, Canadian Cordillera: Elucidating an overprinted geologic history: Geological Society of America Bulletin, v. 111, p. 560–577.

Crowley, J.L., Brown, R.L., and Parrish, R.R., 2001, Diachronous deformation and a strain gradient beneath the Selkirk allochthon, northern Monashee complex, southeastern Canadian Cordillera: Journal of Structural Geology, v. 23, p. 1103–1121, doi: 10.1016/S0191–8141(00)00179–6.

Davis, G.H., and Coney, P.J., 1979, Geological development of the Cordilleran metamorphic core complexes: Geology, v. 7, p. 120–124, doi: 10.1130/0091-7613(1979)7<120:GDOTCM>2.0.CO;2.

Eaton, D.W.S., and Cook, F.A., 1990, Crustal structure of the Valhalla complex, British Columbia, from Lithoprobe seismic-reflection and potential-field data: Canadian Journal of Earth Sciences, v. 27, p. 1048–1060.

Fernández, O., 2005, Obtaining a best fitting plane through 3D georeferenced data: Journal of Structural Geology, v. 27, p. 855–858, doi: 10.1016/j.jsg.2004.12.004.

Gabrielse, H., Monger, J.W.H., Wheeler, J.O., 1991, Tectonic framework; Part A. Morphogeological belts, tectonic assemblages and terranes, *in* Gabrielse, H., and Yorath, C.J., eds., Geology of the Cordilleran Orogen in Canada: Geological Survey of Canada, Decade of North American Geology, no. 4, p. 15–28.

Gervais, F., Brown, R.L., and Crowley, J.L., 2005, Proterozoic strain in the core of the Frenchman Cap dome, Monashee complex; tectonic implications of a strong basement [abs.]: Whitehorse Yukon, Cordillera Tectonics Workshop, p. 10–11.

Ghent, E.D., Nicholls, J., Stout, M.Z., and Rottenfusser, B., 1977, Clinopyroxene amphibolite boudins from Three Valley Gap, British Columbia: Canadian Mineralogist, v. 15, p. 269–282.

Gibson, D., Brown, R.L., and Parrish, R.R., 1999, Deformation-induced inverted metamorphic field gradients: An example from the southeastern Canadian Cordillera: Journal of Structural Geology, v. 21, p. 751–767, doi: 10.1016/S0191–8141(99)00051–6.

Harrap, R.M., 1990, Stratigraphy and structure of the Monashee terrane in the Mount English area, west of Revelstoke, B.C. [M.Sc. thesis]: Ottawa, Ontario, Carleton University, 90 p.

Hobbs, B.E., Means, W.D., and Williams, P.F., 1976, An Outline of Structural Geology: New York, John Wiley & Sons, Inc., 571 p.

Johnson, B.J., 2006, Extensional shear zones, granitic melts, and linkage of overstepping normal faults bounding the Shuswap metamorphic core complex, British Columbia: Geological Society of America Bulletin, v. 118, p. 366–382.

Johnson, B.J., and Brown, R.L., 1996, Crustal structure and early Tertiary extensional tectonics of the Omineca belt at 51°N latitude, southern Canadian Cordillera: Canadian Journal of Earth Sciences, v. 33, p. 1596–1611.

Johnston, D.H., 1998, Structural and thermal evolution of northwest Thor-Odin dome, Monashee complex, southeast British Columbia. [Ph.D. thesis]: Fredericton, New Brunswick, University of New Brunswick, 321 p.

Johnston, D.H., Williams, P.F., Brown, R.L., Crowley, J.L., and Carr, S.D., 2000, Northeastward extrusion and extensional exhumation of crystalline rocks of the Monashee complex, southeastern Canadian Cordillera: Journal of Structural Geology, v. 22, p. 603–625, doi: 10.1016/S0191–8141(99)00185–6.

Jolivet, L., Famin, V., Mehl, C., Para, T., Aubourge, C., Hébert, R., and Philippot, P., 2004, Strain localization during crustal-scale boudinage to form extensional metamorphic domes in the Aegean Sea, *in* Whitney, D.L., Teyssier, C., and Siddoway, C.S., eds., Gneisss Domes in Orogeny: Boulder, Colorado, Geological Society of America Special Paper 380, p. 185–210.

Jones, A.G., 1959, Vernon Map Area, British Columbia: Geological Survey of Canada Memoir 296, 186 p.

Journeay, J.M., 1986, Stratigraphy, internal strain and thermo-tectonic evolution of northern Frenchman Cap dome: An exhumed duplex structure, Omineca hinterland, S.E. Canadian Cordillera [Ph.D. thesis]: Kingston, Ontario, Queens University, 399 p.

Kruse, S., and Williams, P.F., 2005, Brittle faulting in the Thor-Odin culmination, Monashee complex, southern Canadian Cordillera: Constraints on geometry and kinematics: Canadian Journal of Earth Sciences, v. 42, p. 2141–2160, doi: 10.1139/e05–084.

Kruse, S., McNeil, P.D., and Williams, P.F., 2004, A Geological Compilation Map of the Thor-Odin dome: www.unb.ca/frederiction/science/geology/monashee (January 2006).

Kuiper, Y.D., 2003, Isotopic constraints on timing of deformation and metamorphism in Thor-Odin, Monashee complex, southeastern British Columbia [Ph.D. thesis]: Fredericton, New Brunswick, University of New Brunswick, 294 p.

Kuiper, Y.D., Williams, P.F., and Kruse, S., 2006, Possibility of channel flow in the southern Canadian Cordillera; a new approach to explain existing data, *in* Law, R.D., Searle, M.P., and Godin, L., eds., Channel Flow, Ductile Deformation and Exhumation in Continental Collision Zones: Geological Society of London, Special Publication 268, p. 587–609.

Lane, L.S., 1984, Brittle deformation in the Columbia River fault zone near Revelstoke, southeastern British Columbia: Canadian Journal of Earth Sciences, v. 21, p. 584–598.

Lane, L.S., Ghent, E.D., Stout, M.Z., and Brown, R.L., 1989, *P-T* history and kinematic of the Monashee décollement near Revelstoke, British Columbia: Canadian Journal of Earth Sciences, v. 26, p. 231–243.

McNicoll, V.J., and Brown, R.L., 1995, The Monashee décollement at Cariboo Alp, southern flank of the Monashee complex, southern British Columbia, Canada: Journal of Structural Geology, v. 17, p. 17–30, doi: 10.1016/0191–8141(94)E0028-W.

Means, W.D., and Williams, P.F., 1972, Crenulation cleavage and faulting in an artificial salt-mica schist: The Journal of Geology, v. 80, p. 569–591.

Mutti, L.J., 1978, Structure and metamorphism of the Cranberry Region, Thor-Odin gneiss dome [Ph.D. thesis]: Cambridge, Massachusetts, Harvard University. 109 p.

Norlander, B.H., Whitney, D.L., Teyssier, C., and Vanderhaeghe, O., 2002, Partial melting and decompression of the Thor-Odin dome, Shuswap metamorphic core complex, Canadian Cordillera: Lithos, v. 61, p. 103–125, doi: 10.1016/S0024–4937(02)00075–0.

Parrish, R.R., 1995, Thermal evolution of the southeastern Canadian Cordillera: Canadian Journal of Earth Sciences, v. 32, p. 1618–1642.

Parrish, R.R., and Armstrong, R.L., 1983, U-Pb zircon age and tectonic significance of gneisses in structural culminations of the Omineca crystalline belt, British Columbia: Geological Society of America Abstracts with Programs, v. 15, no. 5, p. 324.

Parrish, R.R., Carr, S.D., and Parkinson, D.L., 1988, Eocene extensional tectonics and geochronology of the southern Omineca belt, British Columbia and Washington: Tectonics, v. 7, p. 181–212.

Pumpelly, R., Wolff, J.E., and Dale, T.N., 1894, Geology of the Green Mountains: U.S: Geological Survey Memoir 23, 157 p.

Read, P.D., and Brown, R.L., 1981, Columbia River fault zone: Southeastern margin of the Shuswap and Monashee complexes, southern British Columbia: Canadian Journal of Earth Sciences, v. 18, p. 1127–1145.

Reesor, J.E., and Moore, J.M., 1971, Petrology and structure of Thor-Odin gneiss dome, Shuswap metamorphic complex, British Columbia: Geological Survey of Canada Bulletin, v. 195, p. 1–117.

Spark, R.N., 2001, Crustal thickening and tectonic denudation within the Thor-Odin culmination, Monashee complex, southern Canadian Cordillera [Ph.D. thesis]: Fredericton, New Brunswick, University of New Brunswick, 387 p.

Thompson, R.I., Glombick, P., Acton, S., Heaman, L., Friedman, R.M., Daughtry, K.L., Erdmer, P., and Paradis, S., 2002, New constraints on the age and distribution of the Chase Quartzite, Vernon (82L) and Lardeau (82K) map areas: Regional implications: Slave–Northern Cordillera Lithospheric Evolution (SNORCLE) Transect and Cordilleran Tectonics Workshop Meeting, Lithoprobe Report 82, p. 92–94.

Turner, F.J., and Weiss, L.E., 1963, Structural analysis of metamorphic tectonites: New York, McGraw-Hill Book Company Inc., 545 p.

Varsek, J.L., and Cook, F.A., 1994, Three-dimensional crustal structure of the eastern Cordillera, southwestern Canada and northwestern United States: Geological Society of America Bulletin, v. 106, p. 803–823, doi: 10.1130/0016–7606(1994)106<0803:TDCSOT>2.3.CO;2.

Vasudevan, K., Cook, F.A., and Maier, R., 1995, Three-dimensional seismic structure of the Monashee hinterland core complex on the Lithoprobe Southern Canadian Cordillera Transect: Canadian Journal of Earth Sciences, v. 32, p. 1531–1540.

Williams, P.F., and Jiang, D., 2005, An investigation of lower crustal deformation: evidence for channel flow and its implications for tectonics and structural studies: Journal of Structural Geology, v. 27, p. 1486–1504, doi: 10.1016/j.jsg.2005.04.002.

Yin, A., 2004, Gneiss domes and gneiss dome systems, *in* Whitney, D.L., Teyssier, C., and Siddoway, C.S., eds., Gneiss Domes in Orogeny: Boulder, Colorado, Geological Society of America Special Paper 380, p. 1–14.

Manuscript Received 12 April 2006
Revised Manuscript Received 28 November 2006
Manuscript Accepted 9 December 2006